SCIEPublish

Review

Heterogeneous Catalyzed Electrochemical Conversion of CO_2 through C-N Bond Formation

Yanshuang Gu [1], Zhenghao Lv [1], Lixue Zhou [1], Daming Feng [1,2,3,*] and Chunhua Ge [1,3]

[1] College of Chemistry, Liaoning University, Shenyang 110036, China; 4032332268@smail.lnu.edu.cn (Y.G.); 17860391620@163.com (Z.L.); lxzhou21@163.com (L.Z.); chhge@lnu.edu.cn (C.G.)

[2] State Key Laboratory of Biobased Transportation Fuel Technology, Zhejiang University, Hangzhou 310058, China

[3] Institute of Functional Organic Materials, Liaoning University, Shenyang 110036, China

* Corresponding author. E-mail: dmfeng@lnu.edu.cn (D.F.)

Received: 17 June 2025; Accepted: 7 July 2025; Available online: 16 July 2025

ABSTRACT: The electrocatalytic transformation of carbon dioxide into valuable chemical compounds has gained increasing significance, particularly in the production of nitrogen-containing species via C-N bond formation. This review is organized around the "nitrogen source as the main thread, the product as the branch, and the mechanism as the underlying logic", summarizing and discussing the latest research work on the formation of C-N bonds involving CO_2 under electrochemical conditions. Firstly, these works are classified by the N-containing substrates (oxynitrides, dinitrogen gas, and ammonia) and productions (urea, amines, amides, carbamates, and amino acids). Then, various types of electrocatalysts are demonstrated in depth, including experimental and theoretical results. Finally, the conclusion is presented as well as the future perspectives.

Keywords: CO_2 conversion; Nitrogen fixation; C-N bond formation; Electrosynthesis; Heterogeneous catalysis

1. Introduction

The annual increase in carbon dioxide (CO_2), one of the contributors to global warming, poses a serious threat to human survival and development [1]. Achieving carbon neutrality or net-zero CO_2 emissions is therefore critical for ensuring the sustainable development of human society [2]. To reduce CO_2 emissions, alternative methods should be developed to replace the fossil-fuel-intensive industries, such as heating supply, transportation tools, and chemical manufacturing. Benefiting from renewable energy technology, clean electricity-driven chemical synthesis with abundant feedstocks is one of the promising eco-friendly processes for the plausible eventual innovation of synthetic chemistry [3]. The mild operation conditions, aqueous circumstance adaptation, and device miniaturization and modularization, generally make them more sustainable and convenient replacements for fossil-fuel technologies that require high temperatures and pressures [4].

Among the modern technologies of electrosynthesis, catalytic reduction of CO_2 (CO_2RR) has been claimed to be one of the effective decarbonization strategies [5]. By achieving carbon neutrality or even negative emissions, the CO_2RR has been continuously investigated for its potential to efficiently convert CO_2 into valuable compounds, especially low-carbon fuels, such as alcohols and hydrocarbons [6]. With the prospective development of nanomaterial science, high selectivity of specific products can be achieved with superior efficiency by the accurate construction and precise modification of the heterogeneous catalysts loaded on electrodes [7]. However, it is still challenging to further introduce CO_2 molecules into value-added transformation processes with a broad scope of products, such as long carbon chains or heteroatom-containing molecules. The electrocatalytic CO_2 reduction process should thus incorporate bond-forming events involving atoms other than C, H, and O [8]. The incorporation of nitrogen atoms can lead to the generation of nitrogenous organic compounds, including urea, amines, amides, and amino acids. These substances are particularly valuable owing to their versatile applications in fields such as synthetic chemistry, pharmaceutical research, agricultural science, and aerospace engineering. Integrated nitrogen fixation for CO_2 conversion extends the feasible application of electrosynthesis and provides a new way for CO_2 resource utilization.

https://doi.org/10.70322/gct.2025.10009

Currently, the practical syntheses of these *N*-containing small molecules are dependent on energy-intensive technologies. Urea is thermochemically synthesized by coupling NH_3 and CO_2 at 210 bar and 200 °C, a process known as the Bosch-Meiser urea process. Amines are generated by the amination of alcohols with NH_3 at 100–250 °C and 50–250 bar. Meanwhile, the NH_3 required for these reactions is produced via the Haber-Bosch process, which operates under conditions of 400–500 °C and 100 bar pressure [9]. Although H_2 can be produced through electrochemical water splitting for the Haber-Bosch reaction, these inseparable, multi-step synthetic industries for each product are challenging to decentralize to meet the diversification of modern development.

In recent years, electrochemical nitrogen fixation, such as nitrate reduction [10,11], nitrite reduction [12], and dinitrogen gas reduction [13–16], has been extensively explored. However, most current studies have focused on the preparation of functionalized electrodes and the detection of trace ammonia, while the further processing of the resulting products has rarely been considered. Moreover, the extraction and refinement of ammonia from aqueous solutions pose significant challenges, which limit its potential for practical utilization. Additionally, the products obtained from electrochemical CO_2RR are mostly gases or liquids, which are not convenient for enrichment and subsequent processing, thereby limiting their large-scale and wide applications. Borrowing from the C-C coupling achieved in the electrochemical CO_2RR process to realize C-N coupling, CO_2 can be drawn into the nitrogen fixation process as an abundant raw material, which provides a prospective way for the improvement of nitrogen recycling.

In this Review, the heterogeneous electrochemical catalytic strategies for *N*-containing organic compounds are significantly considered as promising alternatives to the thermochemical processes. While these approaches are still in developmental stages and their underlying reaction mechanisms require further elucidation, a preliminary catalytic system can be established based on known catalytic processes. The initiative mechanism can be provided insight through the summary of these representative cases, and the orientation of further development can be clarified in this field. To this end, several reviews related to the electrochemical co-reduction of CO_2 and nitrogen sources as well as C-N bond formation processes, have been published [17–19]. In this literature, the electrochemical C-N bond formation with CO_2 as one of the reactants was first classified according to the N sources and discussed in terms of major products as well as the type of electrocatalysts. Then, the mechanisms were demonstrated including the co-activation of reactants and the formation of C-N bonds. Several theoretical studies were mentioned to provide solid support for the experimental results. Ultimately, the obtained achievements and remaining challenges were summarised to inspire future advances.

2. Nitrous-Integrated CO_2 Reduction

Nitrogen oxides (NOx), key contributors to acid precipitation, photochemical haze, and ozone layer depletion, pose severe threats to both ecological systems and public health. The accelerated growth of industrial activities, driven primarily by extensive fossil fuel utilization, has led to an exponential increase in anthropogenic NOx emissions, necessitating immediate remedial measures. The electrocatalytic transformation of NOx into high-value nitrogenous compounds represents a dual-purpose approach that aligns with the principles of green chemistry.

2.1. Urea as the Major Product

From 1996 to 2003, Shibata and co-workers conducted a series of pioneering works toward the N-integrated conversion of carbon dioxide under mild electrochemical conditions [20–23]. In their research, various metals (Co, Cr, Mo, Sn, Ag, Cu, Cd, Mn, Ru, Rh, In, Ir, Ni, Pb, Pt, Au, Zn, Tl, and Pd), metal borides (TiB_2, CrB, ZrB_2, NbB_2, MoB, and WB) and metallophthalocyanines (M-Pc, M: Ag, Cr, Mo, Sn, Mn, Rh, Ru, Co, Zn, Pd, Ni, Ir, Tl, Pt, Cu, Au, Cd, In, and Pb) have been adopted as active catalysts and loaded on gas diffusion electrodes for the co-reduction of CO_2 and nitrate or nitrite ions. According to the results, the performance of urea generation is directly related to the efficiency of the sole reduction of CO_2 and nitrate or nitrite. Intriguingly, a linear correlation was found between FE(urea) and $[FE(CO)*FE(NH_4^+)]^{0.5}$ for all three kinds of catalysts (Figure 1a) [24]. Consequently, the generation of C-N bonds was postulated to involve carbon monoxide and ammonia intermediates. Besides, the relatively lower $FE_{(urea)}$ of nitrate-integrated CO_2 reduction compared to the nitrite one at the same potential may be due to the concentration of *in-situ* generated ammonia-like precursor in the reduction of nitrogen oxides.

In recent years, nanostructured materials with specific compositions and surface morphologies have been utilized as working electrodes, driven by the thriving evolution of material chemistry and electrochemistry. Therefore, enhanced efficiency and particular selectivity were achieved in the electrocatalytic processes. Subsequently, as one of the promising electrochemical strategies, the NO_x-integrated electrochemical CO_2 conversion was further developed with

newly designed and fabricated electrocatalytic materials. According to the different types of materials used as catalytic electrodes, the existing achievements related to electrochemical NO_x-integrated CO_2 conversion were organized as follows.

2.1.1. Metal and Alloys

The noble metals were treated as the most robust active elements in catalytic chemistry. Although solemn noble metals did not present an effective performance of simultaneous conversion of NO_x and CO_2 according to Shibata's works, the promoted synthetic efficiency of urea was demonstrated by the modified noble metal-based electrocatalysts. A Te-doped nanocrystalline Pd catalyst was proposed by Feng et al. for the reductive coupling of nitrite and carbon dioxide to produce urea [25]. When the potential was maintained at −1.1 V versus RHE, the urea production exhibited a Faradaic efficiency of 12.2% with a corresponding nitrogen atom utilization rate of 88.7%. Based on the experimental results and DFT calculations, Te doping optimized the adsorption of CO_2/CO and promoted the reduction of NO_2^- to ammonia, thereby providing a convenient condition for gas-reducing and C-N coupling on the interphase for urea formation. The C-N bond was demonstrated to generate between the *CO from CO_2 and *NH_2 from NO_2^- through nucleophilic attack Figure 1b). Through a similar reaction pathway, Liu and co-workers also realised electrochemical NO_2-integrated CO_2 conversion using ultra-thin Au-Cu alloy self-assembled nanofibers as the electrocatalyst [26]. The enhanced FE (24.7%) and superior urea yield rate (64.8 mmol h^{-1} g^{-1}) were mainly attributed to the bimetallic composition, (111)-dominant facets, and 1D-rich defective structures of the material.

Building upon this approach, researchers engineered bimetallic AuPd nanoalloys by embedding palladium into gold nanoparticles, achieving simultaneous electrochemical reduction of nitrate and carbon dioxide for urea production. This catalytic system attained a Faradaic efficiency of 15.6% and a urea generation rate of 3.4 mmol h^{-1} g^{-1} at an applied potential of −0.5 V versus RHE. [27]. The incorporation of Pd into Au nanoparticles precisely controlled the synergistic reduction of CO_2 and NO_3^- and boosted the following C-N coupling between intermediates. Intriguingly, according to the DFT calculation, the hydroxylamine intermediate was confirmed to react with *CO, offering urea with low activation barriers (Figure 1c).

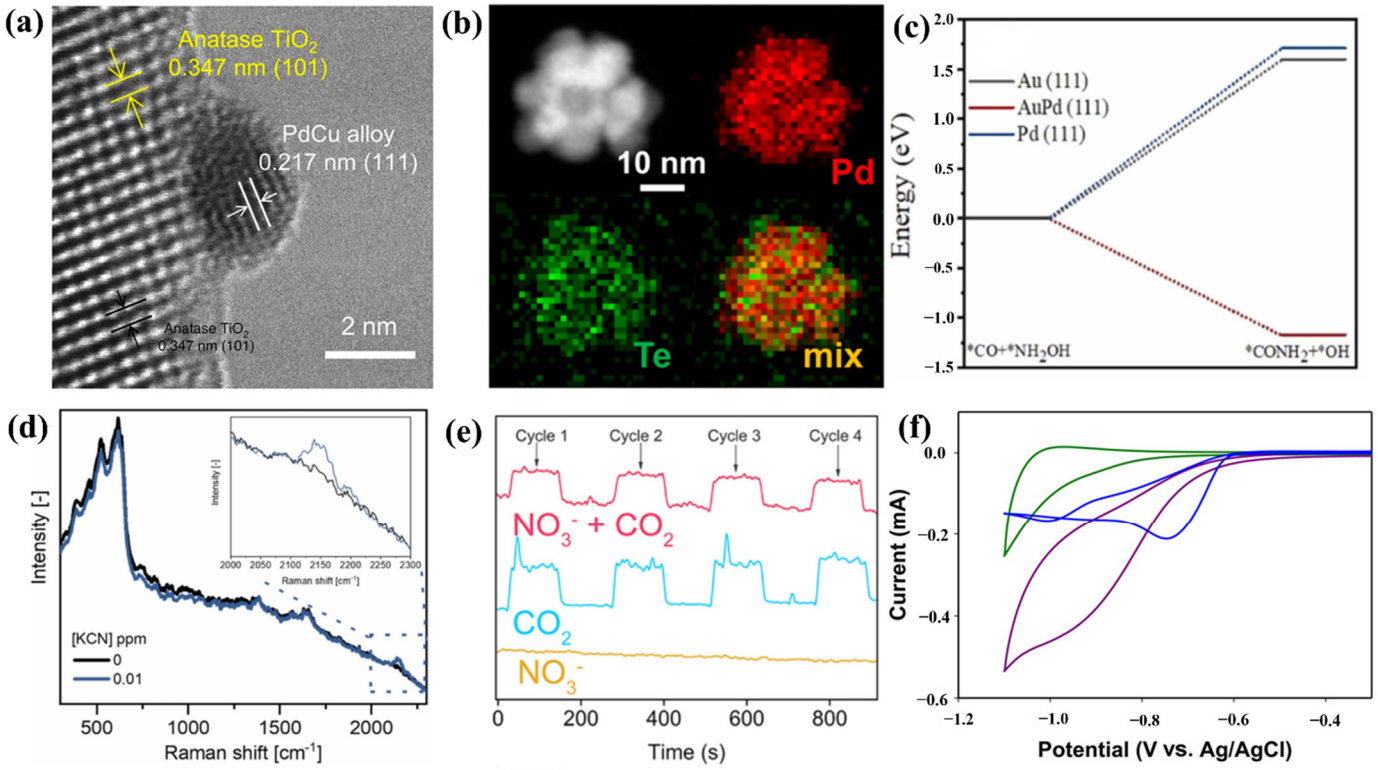

Figure 1. (**a**) High-resolution transmission electron microscopy (HR-TEM) image of PdCu/TiO [24]. Reproduced with permission. Copyright 2020 Springer Nature Limited. (**b**) HAADF-STEM image and elemental distribution profiles of Te-Pd NCs [25]. Reproduced with permission. Copyright 2020, ACS Publications. (**c**) Free energies for *CO+*NH_2OH→*$CONH_2$ on Pd, AuPd, and Au. In situ surface-enhanced Raman spectroscopy (SERS) of a Cu surface in CO_2 saturated 0.1 M $KHCO_3$ at OCV with the addition of KCN [27]. Reproduced with permission. Copyright 2022 Elsevier Publications. (**d**) With 0.01 and 0 ppm of KCN [28]. Reproduced with permission. Copyright 2022, Elsevier Publications. (**e**) Online DEMS spectra of CO signals over Cu@Zn [29].

Reproduced with permission. Copyright 2022, ACS Publications. (**f**) Cyclic voltammetric responses of a TiO_2-Nafion-modified ITO electrode (0.5 cm × 3.5 cm) in 0.1 m KNO_3 (pH 4.5) under Ar atmosphere (green), CO_2 (purple), and bare ITO under CO_2 (blue) at 50 mV s^{-1} scan rate [30]. Reproduced with permission. Copyright 2017, WILEY Publication.

Because of the mysterious coupling function of Cu for the electrosynthesis of multi-carbon products in CO_2RR, Cu-based catalysts were considered one of the most promising candidates in electrochemical C-N coupling reactions [31,32]. Krzywda's team has previously reported that the electrodeposition of copper on a Cu-Ti electrode leads to the NO_3—integrated reduction of CO_2 for the production of urea [28]. SERS successfully identified the establishment of C-N covalent bonds through the coupling of $*NH_2$ and *CO intermediates on the copper electrocatalyst surface. The comparison of Raman spectra demonstrated that C-N coupling was formed on the surface of the Cu, not the residual Cu_2O during the process of electrolytic reduction, generating a unique cyanide intermediate (Figure 1d). Although the FE of urea is relatively low in this work, a novel reaction pathway was proposed. To enhance the catalytic performance of a Cu electrode in the electrosynthesis of urea, Meng et al. constructed self-supporting core-shell Cu@Zn nanowires through electroreduction and applied to electrochemical NO_3^--integrated reduction of CO_2 in an aqueous solution [29] (Figure 1e). Under the condition of −1.02 V *vs.* RHE, the urea yield rate and FE reached 7.29 μmol·cm^{-2}·h^{-1} and 9.28%, respectively. Employing means of online DEMS, DFT analysis, and in situ ATR-FTIR, the catalytic mechanism was proven similar to that of Te-doped Pd and AuCu. The electron donation from the zinc shell to the copper core promoted the generation and subsequent coupling of *CO and $*NH_2$ intermediate species.

Apart from Cu-based materials, other transition metals also possess the ability to trigger the electrosynthesis of urea after elaborate fabrication. Under environmental conditions, urea was formed through electrochemical NO-integrated reduction of CO_2 catalyzed by zinc nanobelts constructed by in-situ electrochemical reduction of ZnO nanosheets [33]. As an active nitrogen source and one of the crucial intermediates in the electrochemical reduction of nitrite/nitrate, NO facilitated the conversion of CO_2 into urea with less electron and proton demand. A flow cell with gas diffusion layer electrodes and a peristaltic pump further enhances the urea yield rate and FE at 15.13 mmol·h^{-1}·g^{-1} and 11.26%, respectively. According to theoretical calculations, the C-N bond formation took place between $*NH_2$ and *CO intermediates.

2.1.2. Metal Oxides and Hydroxides

The semiconductive metal oxides and hydroxides exhibited particular catalytic performance for mediating the electrochemical conversion of inert small molecules. Due to the unique adsorption ability and the intrinsic defects on the surface, CO_2 can be accumulated and activated at the interface of the electrode and electrolyte. A homogeneous porous TiO_2-Nafion composite electrode has been investigated by Shin and co-workers for the electrochemical simultaneous reduction of CO_2 and NO_3^- under mild reaction conditions [30] (Figure 1f). The urea was produced along with CO, NH_3, and H_2 as by-products, and 40% of FE_{urea} was calculated according to the experimental data. Furthermore, nanostructured $FeTiO_3$ composites demonstrated notable catalytic activity toward urea electrosynthesis during CO_2 reduction coupled with NO_2^- incorporation [34] (Figure 2b). Recent work by Anastasiadou and Figueiredo (2024) revealed that CuO_xZnO_x catalysts achieve a 41% Faradaic efficiency at −0.8 V *vs.* RHE, attributed to electron transfer between Cu/Zn sites, which lowers the energy barrier for CO–NH_2 coupling. This exemplifies how bimetallic design enhances interfacial charge transfer for C–N bond formation [35].

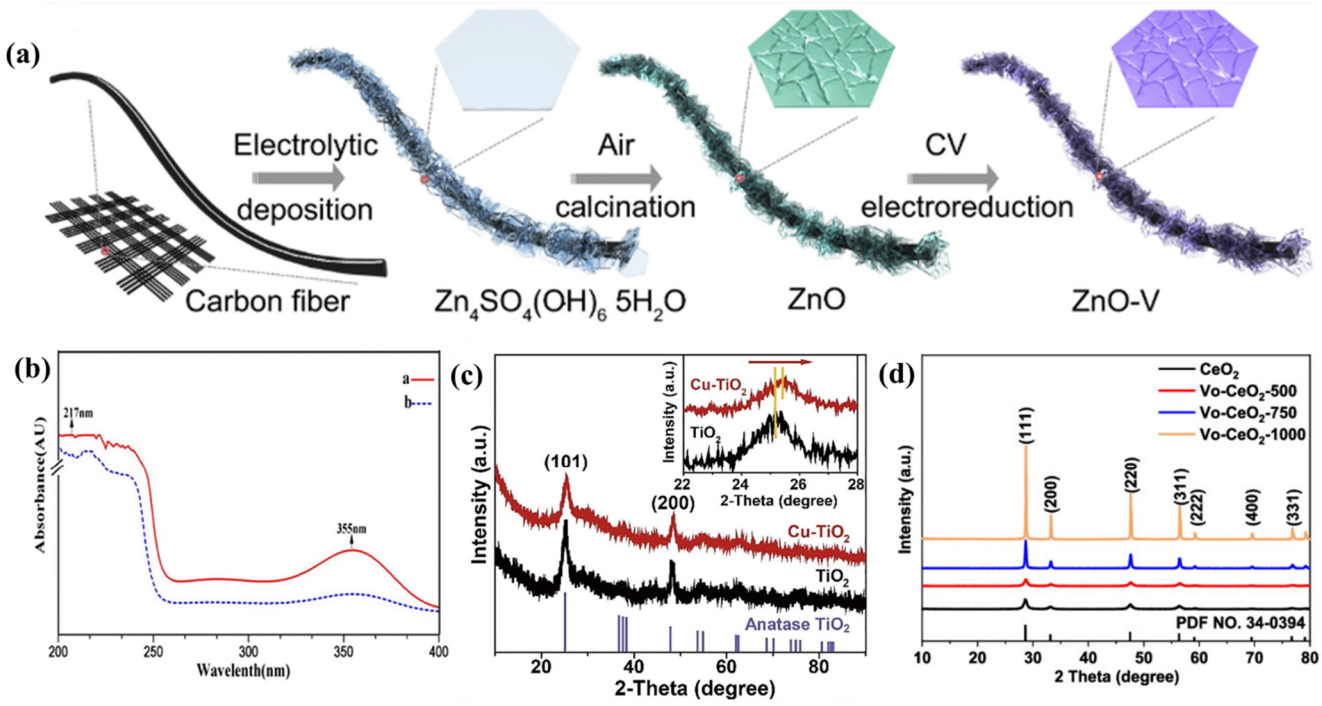

Figure 2. (**a**) Synthetic procedure illustration of the synthesis of ZnO-V porous nanosheets [36]. Reproduced with permission. Copyright 2021 Elsevier Publication. (**b**) UV-vis absorption spectra of graph *a* microwave-synthesized and graph *b* co-precipitate synthesis $FeTiO_3$ of CO_2 saturated 0.2 M KNO_2 and 1 M $NaHCO_3$ solution after reduction [34]. Reproduced with permission. Copyright 2017 Springer Nature Limited. (**c**) X-ray diffraction (XRD) patterns result for undoped TiO_2 (black) and Cu-TiO_2 (red). Inset: the enlarged view of the XRD pattern at 22°–28° range. The yellow lines indicated the positions of the corresponding peak positions. The red arrow indicates that the XRD peaks of the Cu-TiO_2 sample gradually shift to higher diffraction angles [37]. Reproduced with permission. Copyright 2020 Elsevier Publication. (**d**) XRD patterns of Vo-CeO_2-1000, Vo-CeO_2-75, Vo-CeO_2-500, and CeO_2. Reproduced with permission. Copyright 2022, ACS Publication.

As one of the useful defects, oxygen vacancy (V_O) was certificated to promote the catalytic performance in various electrochemical conversion reactions. For the reductive coupling of CO_2 and nitrite, Cao et al. constructed an oxygen vacancy-rich anatase TiO_2 with low-valence Cu-dopant (Cu-TiO_2-V_o) as the electrocatalysts for the synthesis of urea [37] (Figure 2c). The oxygen vacancies in TiO_2 and Cu were instrumental in adsorbing NO_2^- and CO_2 and generating $*NH_2$ and *CO intermediates, respectively. After the following C-N bond formation, a FE of 43.1% (at −0.4 V *vs.* RHE) was attained for urea synthesis. Similarly, an oxygen vacancy-rich ZnO (ZnO-V) nanosheet was also used as a self-supporting electrode by Meng et al. for the electrosynthesis of urea from CO_2 and NO_2^- [36] (Figure 2a). Compared to the pristine ZnO, the oxygen vacancies in the porous ZnO nanosheets further enhanced the electrocatalytic performance towards urea production, with FE increasing from 8.10% to 23.26% (at −0.79 V *vs.* RHE).

Furthermore, the introduction of oxygen vacancies was also demonstrated to boost the electrochemical CO_2 conversion with NO_3^- (Figure 2d). By fine-tuning the concentrations of V_O on the CeO_2 nanorods, urea can be provided with 15.7 $mmol \cdot h^{-1} \cdot g^{-1}$ at −1.6 V *vs.* RHE [38]. Based on the validation of in situ SFG spectroscopy and theoretical calculations, V_O can stabilize the reactive intermediates and facilitate selective C-N bond formation. The coupling reaction took place between *CO and *NO after the reduction of CO_2 and NO_3^-, yielding *OCNO intermediate. After subsequent alternating protonation, the urea was generated and desorbed from the electrode surface.

Indium hydroxides have been proven effective in the electrochemical conversion of CO_2. Lv and co-workers proposed an $In(OH)_3$ with (100) facet exposure ($In(OH)_3$-S) prepared by solvothermal methods for the electrosynthesis of urea [39]. The conversion of CO_2 with NO_3^- was facilitated by the suppression of competing hydrogen emission reactions due to the type of semiconducting behavior change on the $In(OH)_3$ surface (Figure 3a). With the aid of Mott-Schottky measurements, a definite transformation of n-type to p-type semiconductors can be deduced. An ultrahigh FE_{urea} of 53.4% was obtained at −0.6 V *vs.* RHE, and the selectivity of C and N was 82.9% and 100% respectively, because the formation of the solemn nitrogen-containing or carbon-containing by-products was mostly inhibited depending on the facet activity. DFT simulations combined with operando synchrotron radiation FTIR spectroscopy revealed that C-N bond formation between $*CO_2$ and $*NO_2$ intermediates likely initiates at the early reaction stage on $In(OH)_3$ crystal facets. Furthermore, the $*CO_2NH_2$ intermediate was formed through protonation, and the generation of

urea was realized after a second C-N coupling with $*NO_2$ and further protonation. As a continuation, the indium oxyhydroxide with oxygen vacancy ($InOOH\text{-}V_O$) was also solvothermal fabricated and displayed selective C-N coupling toward electrochemical NO_3^--integrated CO_2 conversion, providing urea as the major product with 51% FE [40]. The oxygen vacancies were verified to facilitate early-stage C-N bond formation and the following protonation processes by regulating the local electronic structure of the surface-active atom (Figure 3b).

2.1.3. Single Atomic Catalysts

Benefiting from maximum atomic utilization and defined activity centers, single atomic catalysts exhibit significantly enhanced catalytic activity in a variety of reactions. For example, using sodium chloride as a template, a highly dispersed copper monatomic catalyst was prepared for the simultaneous reduction of CO_2 and NO_3^- under electrochemical conditions [41] (Figure 3c). The freeze-drying technique prevented the aggregation of copper. And the single-atom state of copper was validated by HAADF-STEM images. Revealed by the XAS and XANES spectra, the two different coordination structures of Cu in the catalytic SAC material, that is $Cu\text{-}N_4$ and $Cu\text{-}N_{4-x}\text{-}C_x$, synergistically promoted the co-reduction of CO_2 and NO_3^-. Based on the DFT calculations, the coupling of *CO and $*NH_2$ intermediate occurred at a relatively late stage after the reduction.

In 2022, Zhang's research team demonstrated that bimetallic Fe-Ni dual-atom catalysts (B-FeNi-DASC) could remarkably enhance urea electrosynthesis efficiency, achieving a production rate of 20.2 mmol h^{-1} g^{-1}. [42]. A relatively higher FE of 17.8% was also obtained by the catalysis of B-FeNi-DASC, compared with that of single metal and isolated bimetal catalysts. By combining the active site and the coupling site, the bonded Fe-Ni diatoms effectively promoted the NO_3^- and CO_2 activation, as well as the C-N coupling processes. The theoretical calculation shows that the B-FeNi-DASC can adsorb and reduce the *NO at a low energy level, generating *NH intermediate. The operando SR-FTIR measurements demonstrated that the key intermediate *NHCONO was formed by the direct coupling of *NH and*CO and a rapidly second *NO connection. The urea was formed subsequently by the PCET process with *NHCONO (Figure 3d).

2.2. Other Organo-Products

In addition to urea, organic amines can also be available through electrochemical NO_x-integrated CO_2 conversion. A molecular electrocatalyst hybridized by β-tetra-aminophthalocyanine cobalt and carbon nanotube ($CoPc\text{-}NH_2$/CNT) was synthesized for electrochemical NO_3^--integrated CO_2 conversion [43]. After the characterization towards yielding products in the gas or liquid phase, methylamine was detected as the most abundant molecule among C-N coupling products. Catalyzed by the active CoPc sites, the $*OCH_2$ and $*OHNH_2$ were reductively generated by CO_2 and NO_3^- respectively, within which $10e^-$ and $11H^+$ were transferred (Figure 3e). A possible route of methylamine formation was elucidated through a series of control experiments, and formaldoxime was identified as the key intermediate, which may be generated from the condensation of hydroxylamine and formaldehyde intermediates. In another study from the same group, ethylamine products can be obtained through the electrochemical co-reduction of CO_2 and NO_3^- catalyzed by Cu-base heterogeneous catalysts [44]. During the electrolysis, the CO_2 was transformed to adsorbed acetaldehyde through 8e reduction and a C-C bond formation process, while the NO_3^- was converted to a bounded hydroxylamine intermediate through $6e^-$ reduction. Similar to the formation of methylamine in the formal study, acetaldoxime was formed through the C-N coupling of acetaldehyde-hydroxylamine condensation. After following reduction and protonation, ethylamine was eventually yielded and can be accumulated by long-time electrolysis.

As one of the promising offerings from electrochemical CO_2RR, formic acid has received widespread attention and has been achieved at a pilot plant scale. As an alternative to direct electrochemical NO_x-integrated CO_2 conversion, Guo and co-workers proposed an electrosynthesis of formamide through the CO_2-derived HCOOH coupling NO_2^- co-reduction process [45] (Figure 3f). Derived from Cu_2O nanocubes by electrochemical reduction, the low-coordinated Cu nanocubes exhibited superior catalytic performance for formamide products with 29.7% FE at −0.4 V *vs.* RHE. The C-N bond was generated via condensation coupling of *CHO and $*NH_2$, which were verified by the *in-situ* spectra and theoretical calculations. Furthermore, the developed electrochemical approach enables efficient conversion of acetic acid to acetamide.

In addition, the reductive C-N bond formation was achieved between nitrate ions and oxalic acid that originated from CO_2 reduction [46]. After verification of the ^1H NMR, the glycine was detected as the most valuable C-N coupling product.

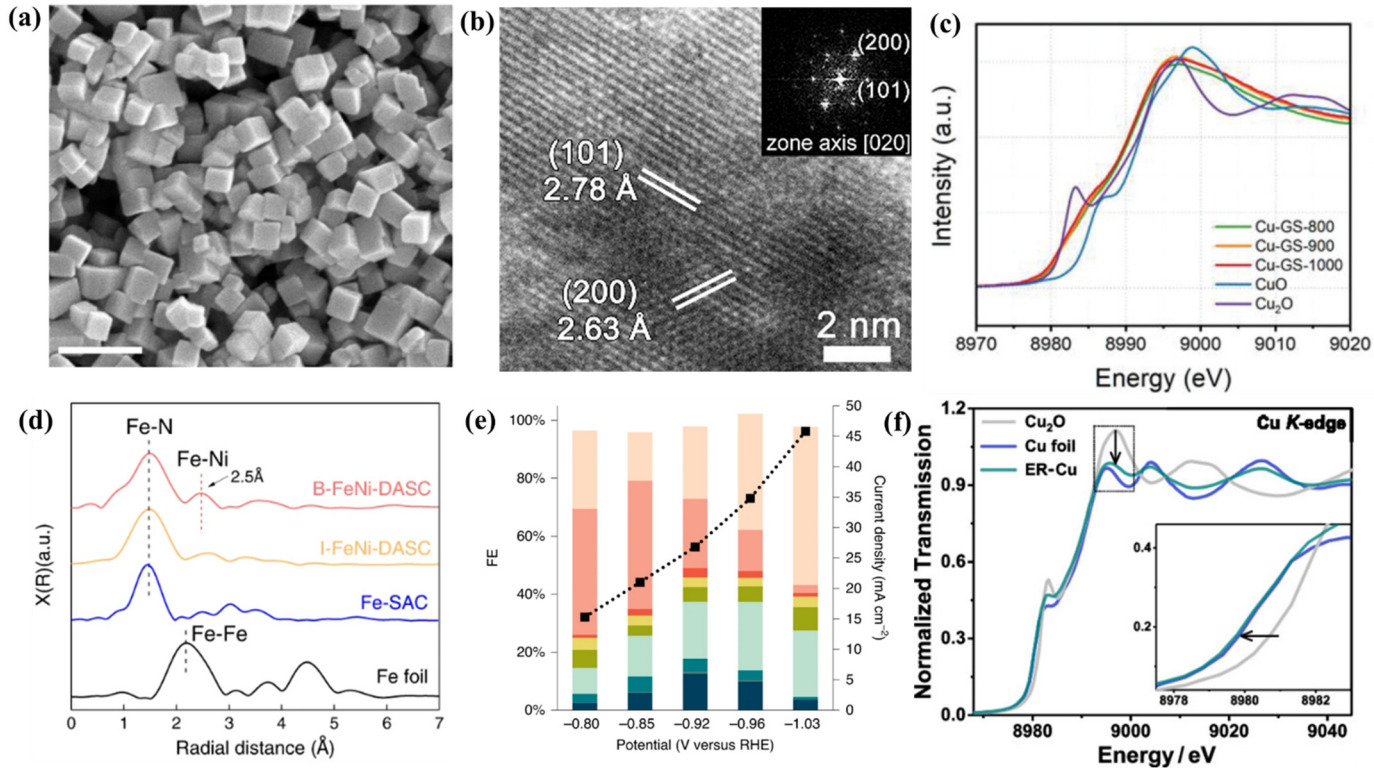

Figure 3. (**a**) Scanning Electron Microscope (SEM) image of $In(OH)_3$-S, Scale bars in are 500 nm (unit for reciprocal space) [39]. Reproduced with permission. Copyright 2021 Springer Nature Limited. (**b**) HR-TEM images of V_O-InOOH [40]. Reproduced with permission. Copyright 2022, ACS Publication. (**c**) X-ray absorption near-edge structure (XANES) spectra at Cu K-edge for as-synthesized Cu-GS-1000, Cu-GS-900, and Cu-GS-800, compared to reference $Cu^{II}O$ (Cu(II)) [41]. Reproduced with permission. Copyright 2022, WILEY Publication. (**d**) Fourier transform extended X-ray absorption fine structure (FT-EXAFS) spectra of B-FeNi-DASC, I-FeNi-DASC, and Fe-SAC [42]. (**e**) Potential-dependent product distribution (FE) and total current density [43]. (**f**) Cu K-edge extended XANES spectra of Cu_2O, Cu foil, and ER-Cu [45]. Reproduced with permission. Copyright 2021, 2021 Springer Nature Limited.

3. Dinitrogen-Integrated CO_2 Reduction

As the most abundant gas in the atmosphere, nitrogen is used in a variety of natural and artificial nitrogen fixation processes. However, these processes either cannot be mass-produced industrially or are energy-intensive, which has an adverse effect on the development of human beings. Meanwhile, the emerging photo- or electro-chemical mediated fixation of N_2 is limited by low conversion efficiency and production enrichment difficulties for practical use [47–50]. As a promising alternative, carbon dioxide and nitrogen can be co-reduced and coupled to form C-N bond-containing products under electrochemical conditions (Figure 4a). The challenging adsorption of both gas substrates and the subsequent C-N formation requires precise construction of functional materials and fine-tuning of surface electronic distribution, and there have been several successful cases [51]. To date, the only product formed through C-N coupling is urea. The following content was discussed in relation to different types of electrocatalysts and methods adopted to enhance the reactive efficiency and catalytic selectivity.

3.1. Metallic Alloys

Alloys, one of the robust catalysts with outstanding synergic effects in various catalysis, also presented robust catalytic performance in electrochemical N_2-integrated CO_2 conversion. As a unique catalytic site, Cu is claimed to possess a coupling function during the catalysis process, proven by various electrochemical CO_2RR toward C2 production [52]. Therefore, introducing Cu element into alloy materials is promising in boosting electrochemical C-N coupling reactions. In addition, defect engineering is crucial for such alloy catalysts in aqueous electrochemical reactions, due to the indispensable enhancement of adsorption of insoluble feed gases. In 2020, Chen and co-workers used PdCu nanoparticles loaded on titanium dioxide to electrocatalyst the reduction and coupling of N_2 with carbon dioxide to form urea. −0.4 V *vs.* RHE [53]. The system achieved a urea production rate of 3.36 mmol g^{-1} h^{-1} with a FE of 8.92%. The incorporation of alloy nanoparticles was found to strengthen nitrogen and carbon dioxide adsorption,

thereby improving the overall catalytic performance (Figure 4b). Due to the bimetallic synergistic effect and electronic optimization, the catalyst exhibits superior catalytic activity, enabling carbon-nitrogen coupling to form urea. The composite material exhibited a dual function in the co-reduction of CO_2 and N_2, and the C-N bond formation was further boosted by the Cu counterparts in the alloy. Recently, through the chemical reduction of a mixture of ammonium bismuth citrate and copper chloride, a defective Cu-Bi alloy was synthesized and utilized as electrocatalysts in the co-reduction of N_2 and CO_2 (Figure 4c) by Wu et al. [54].

3.2. Hybrid Materials

Heterojunction nanomaterials possess a dual active site, exhibiting synergistic effects on electrocatalytic transformations. On the surface of well-defined catalytic materials, nucleophilic and electrophilic sites are dispersed, which not only facilitates the adsorption and activation of inert gases such as N_2 and CO_2 but also promotes the subsequent coupling process between reduced intermediates. In this context, Yuan and co-workers designed several hetero-structured nano-materials to enhance C-N bond formation towards the generation of urea. The well-designed Bi-based Mott-Schottky heterostructure (Bi-$BiVO_4$) [55] (Figure 4d) and the perovskite hybrids ($BiFeO_3$-$BiVO_4$) [56] (Figure 4e) were fabricated and applied in the electrochemical conversion of N_2 and CO_2 into urea under ambient conditions. At −0.4 *vs.* RHE in 0.1 M $KHCO_3$, the FE of urea was 12.55% and 17.18%, respectively. In both cases, The $BiVO_4$ acted as the electrophilic catalytic site, which adsorbed the N_2 molecule with a side-on configuration (*N=N*). According to the free energy calculation, the side-on bound N_2 was more stable and negative than the end-on configuration. Additionally, CO_2 molecules undergo adsorption and activation at the nucleophilic Bi/$BiFeO_3$ interfaces, resulting in the formation of the key *CO intermediate. Subsequently, the C-N coupling occured between the negative *N=N* intermediate and the positive *CO intermediate, yielding *NCON* with relatively low energy barriers. The formation of urea preferentially underwent the distal protonation process. The catalytic performance can be further promoted by introducing an ionic liquid electrolyte to enhance CO_2 solubility in the system.

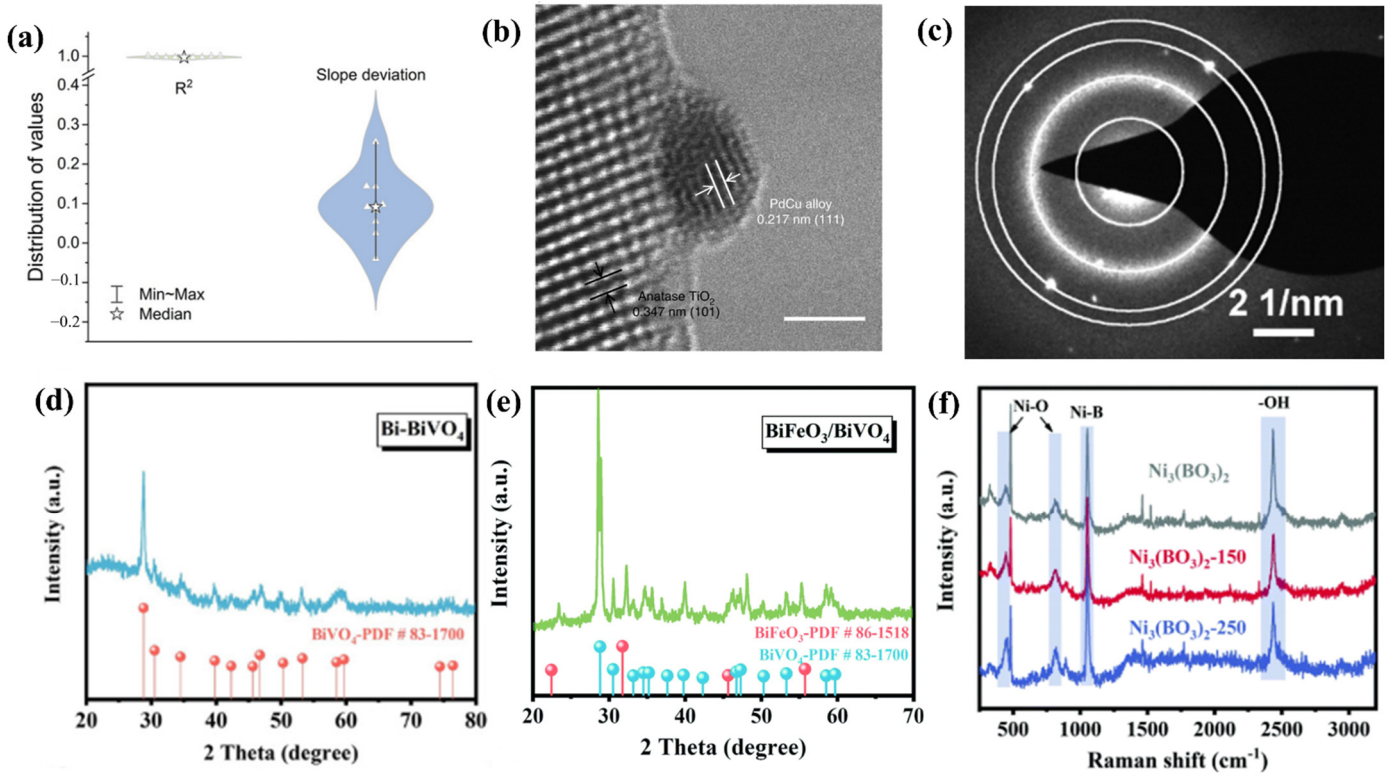

Figure 4. (**a**) The distributions of R^2 and slope deviation under all tests by the urease method [51]. Reproduced with permission. Copyright 2022, WILEY Publication. (**b**) HR-TEM image of Pd_1Cu_1/TiO_2-400. Scale bar: 2 nm. Reproduced with permission. Copyright 2020 Springer Nature Limited. (**c**) Selected area electron diffraction (SAED) of defective Cu-Bi. Each circle represents the collection of the same crystal plane of different crystal grains [54]. Reproduced with permission. Copyright 2022 Elsevier Publication. (**d**) XRD patterns analysis of Bi-$BiVO_4$ [55]. Reproduced with permission. Copyright 2021, WILEY Publication. (**e**) XRD pattern analysis of $BiFeO_3/BiVO_4$ [56]. Reproduced with permission. Copyright 2021, RSC Publication. (**f**) Raman spectra of the pristine $Ni_3(BO_3)_2$-250, $Ni_3(BO_3)_2$-150, and $Ni_3(BO_3)_2$ catalysts [57]. Reproduced with permission. Copyright 2008, RSC Publication.

Furthermore, by fine-tuning the electron distribution and functional modifying components, transition-metal-based materials exhibit incomparable electrocatalytic performance for the selective activation of reactant molecules and C-N coupling ability in urea synthesis. Following a similar synthetic pathway to urea as the Bi-based heterostructures, artificial frustrated Lewis pairs (FLPs) have been demonstrated to be the superior catalysts for electrochemical co-reduction of CO_2 and N_2 for urea production through C-N bond formation. The surface electrostatic potential analysis has demonstrated the positive effect of artificial FLPs on adsorption, activation, and C-N coupling reaction steps during the electrochemical urea synthesis (Figure 4f). Both CO_2 and N_2 can be firmly absorbed and smoothly activated by the neighboring Lewis acid and base active sites. Conspicuously, the C-N coupling can be facilitated through σ-orbital carbonylation strategy by the empty e_g orbital of the catalytic metal site at a low-spin stat (Figure 5). As a proof of concept, a flower-like nickel borate was fabricated and applied to the electrosynthesis of urea, where adjacent Ni atom and hydroxyl group served as Lewis acid and base, respectively [57]. The annealing treatment introduced low-spin Ni^{2+} sites and adjacent hydroxyl groups, achieving a FE of 20.36% at −0.5 V *vs.* RHE and a urea yield rate of 9.70 $mmol \cdot h^{-1} \cdot g^{-1}$. In addition, a rice-like InOOH nanocrystal was also constructed, modified by annealing treatment, and utilized as the catalytic electrode for the N_2-integrated CO_2 conversion into urea, with 20.97% of FE and 6.85 $mmol \cdot h^{-1} \cdot g^{-1}$ of yield rate [58] (Figure 6a). In another example, a conductive MOF Co-PMDA-2-mbIM with host-guest molecular interaction attained the highest FE of 48.97% to date in the electrosynthesis of urea with N_2 and CO_2 [59] (Figure 6b). The guest molecules were demonstrated to regulate the spin-state of Co, providing an empty e_g orbital as the electrophilic region that facilitated the reduction of N_2. After the reduction of CO_2 at the neighboring nucleophilic region, the C-N coupling was triggered through the σ-orbital carbonylation strategy that was mediated by the empty e_g orbital of Co as well. More recently, a Cu-based MOF, Cu-HHTP, (Figure 6c) was also verified as an effective and robust electrocatalysts for the co-reduction of CO_2 and N_2 for the synthesis of urea [60]. After regulation of spin-state through the oxidation of isolated Cu species in the MOF, the catalytic performance was enhanced, obtaining a FE of 23.09% at −0.6 V *vs.* RHE and a high urea yield of 7.780 mmol h^{-1} g^{-1}. The empty d orbitals exhibited superior activation effect for the inert N_2 molecules and the low spin-state favorably promoted the C-N coupling process, thus improving the outstanding synthetic performance toward electrochemical urea production.

Due to the perspective achievement of metal phthalocyanine-based materials [61] in both electrochemical CO_2RR and N_2RR, copper phthalocyanine nanotubes (CuPc NTs) were constructed by Mukherjee and co-workers for electrochemical generation of urea from N_2 and CO_2 [62] (Figure 6d). Thanks to the multiple active sites of CuPc, the CuPc NTs exhibited the FE of 12.99% at −0.6 V *vs.* RHE and the urea yield rate of 143.47 μg h^{-1} mg_{cat}^{-1}. The experimental results and DFT calculations show that the pyridinic-N1 and Cu sites were responsible for CO_2 and N_2 reduction, respectively.

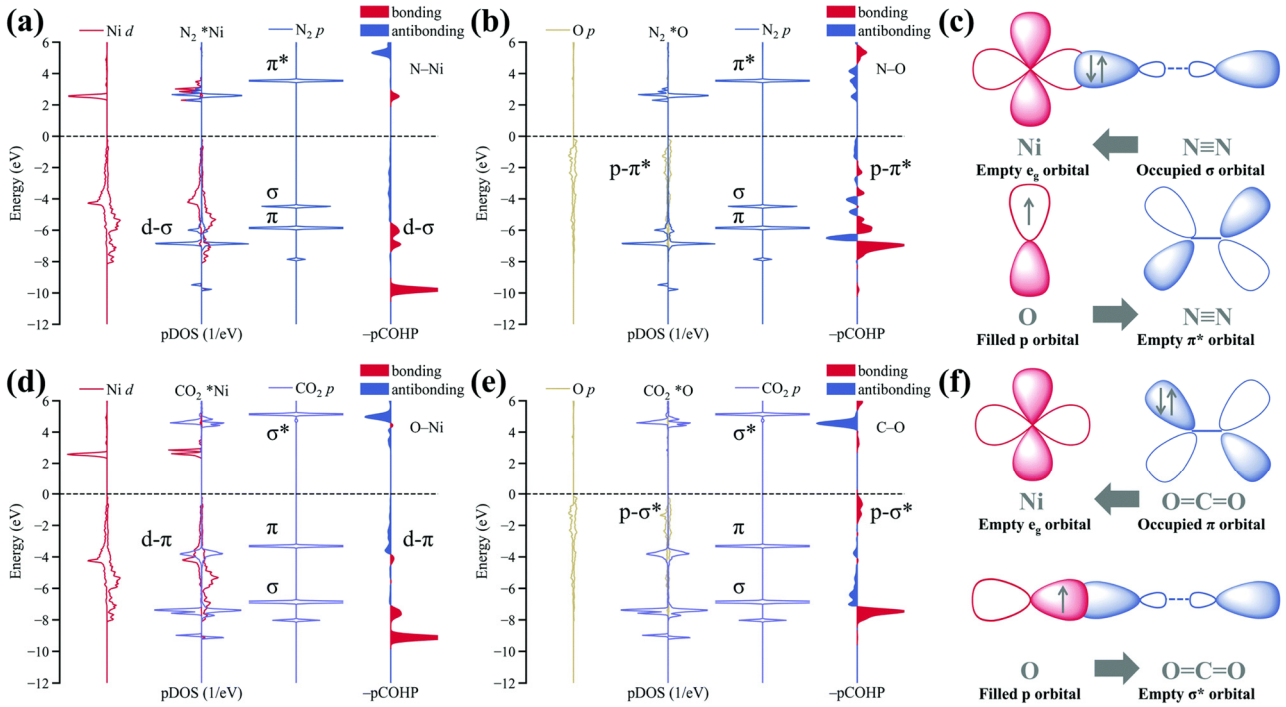

Figure 5. (**a**,**b**) Projected density of states (pDOS) profiles for N_2 adsorption on (**a**) the Ni Lewis acid center and (**b**) the O Lewis base site (within OH^- groups) of engineered frustrated Lewis pairs (FLPs), accompanied by crystal orbital Hamilton population

(pCOHP) analyses of (**a**) Ni-N and (**b**) O-N bonding interactions (right panels), elucidating the gas activation mechanism. (**d**,**e**) Corresponding pDOS spectra for CO_2 binding at (**d**) Ni and (**e**) O sites, with pCOHP evaluations of (**d**) Ni-O and (**e**) C-O bond formation (right panels). Schematic representations depict the charge transfer processes between FLPs and (**c**) N_2 or (**f**) CO_2 molecules, highlighting donor-acceptor interactions. An asterisk "*" before an element symbol indicates that the element is an adsorbed atom on the adsorption site, not an atom of the substrate material itself. The "*" in the superscript of a Greek letter represents an antibonding orbital [57]. Reproduced with permission. Copyright 2008, RSC Publication.

3.3. Composite Methods

To overcome the poor aqueous solubility of N_2 and CO_2, electrochemical N_2-integrated CO_2 reduction at high pressure can be a viable option to enhance the catalytic performance. In 2016, Kayan and co-workers fabricated a Pt electrode covered with conductive polymers for N_2-integrated CO_2 reduction [63]. Under the relatively high pressure of the given gas, namely 30 bar CO_2 and 30 bar N_2, the C-N coupling product was obtained as urea with more PPy coated on the electrode in an aqueous solution (Figure 6f). The chemically generated ammonium carbamate, produced under high pressure, was supposed to be the key intermediate for producing urea, thus the production of urea is primarily related to ammonia that in-situ formed from N_2 reduction.

It has been widely recognized that photochemical assistance can significantly enhance electrocatalytic activity. In this context, Bharath and co-workers proposed a plasmon-enhanced photo-electrochemical process for CO_2 and N_2 into urea [64]. The plasmonic Au nanostructures were synthesized, optimized, and adopted as catalytic materials. Upon visible and near-infrared light illumination, the Au-based electrocatalyst exhibited significantly improved activity, achieving a urea production rate of 98.5 μg h^{-1} $mgcat^{-1}$ with 22.7% Faradaic efficiency at −0.7 V *vs.* RHE (Figure 6e).

3.4. Theoretical Study

To address the challenging problems in the electrocatalytic synthesis of urea from N_2 and CO_2 co-reduction under mild reaction conditions, DFT computations were carried out based on first-principles via the Vienna ab initio simulation package (VASP). The projector-augmented wave (PAW) approach and PBE-GGA functional were employed to characterize ion-electron interactions and exchange-correlation effects, respectively. With a rectangular lattice and planar anisotropic structure, the conductive 2D MBenes (Mo_2B_2, Ti_2B_2, and Cr_2B_2) were theoretically revealed by Li et al. as efficient electrocatalysts for urea synthesis [65]. Based on the calculation result, the urea synthetic pathway was deduced to start from N_2 adsorption with a side-on configuration and the CO_2 binding to the neighboring bridge site. Then, the C-N bond was subsequently formed between the $*N_2$ and *CO intermediate, generating *NCON as the key intermediate. At last, the urea was obtained after alternative hydrogenation steps. It is worth noting that urea desorption was an endothermic process, not the exothermic process reported by the experimental electrocatalysts mentioned above. Another planar CuB_{12} monolayer was investigated and claimed as a promising catalyst for the electrosynthesis of urea through the *NCON hydrogenation as well. After a thoroug exploration of the possible reaction mechanism for urea production, the C-N bond formation was released between *CO and *NHNH intermediates rather than the *NCON pathway [66]. Meanwhile, conductive dual-Si doped g-C_6N_6 nanosheets [67] and a vanadium/nitrogen co-doped carbon nanocrystal [68] were revealed to be highly efficient for electrocatalytic urea generation from N_2 and CO_2 through the *NCON hydrogenation pathway. More recently, an atomic dispersed dual-metal catalyst constructed on N-doped graphene, namely $M_2@N_6G$, was theoretically studied for latent application in the electrosynthesis of urea [69]. After systematical exploration, 8 optimized catalytic materials were verified to promote the C-N coupling reaction through the *NCON pathway. The principal descriptor (ΔE(*NCONH)) was demonstrated for future evaluation of the investigation of the electrosynthesis of urea.

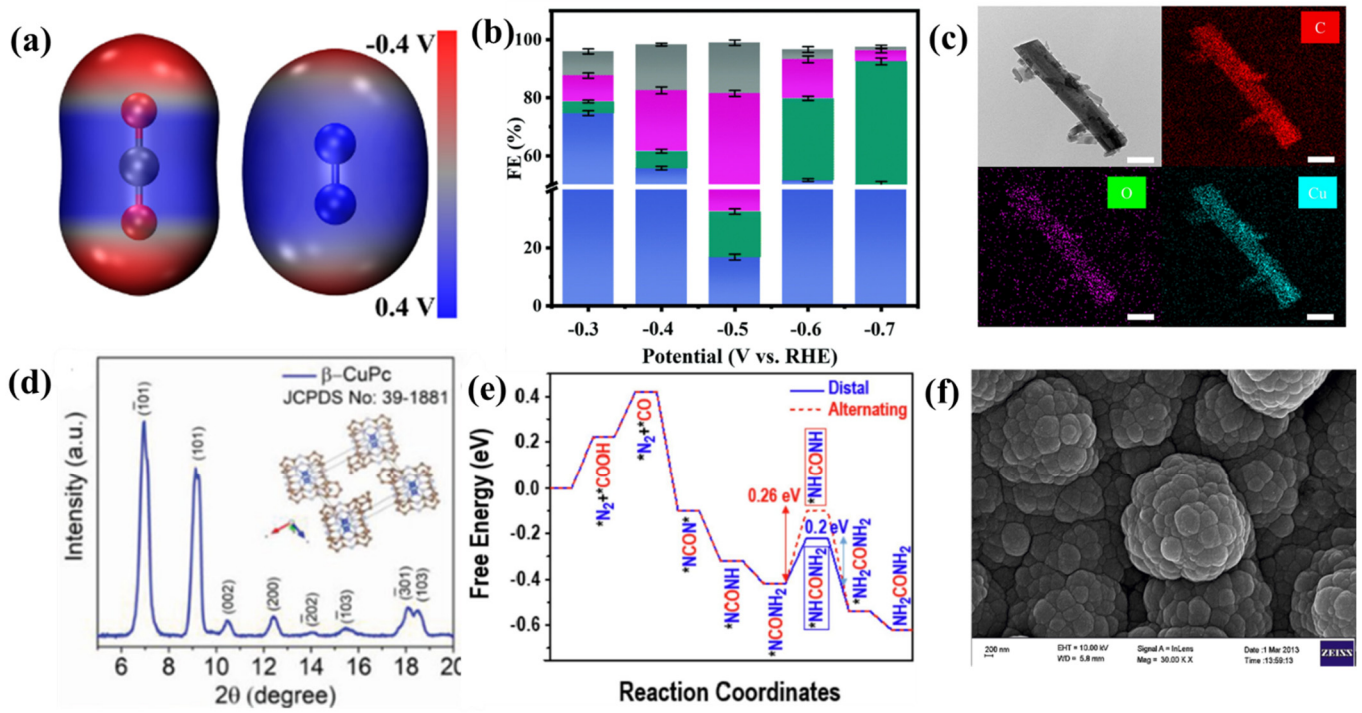

Figure 6. (**a**) Electron-density isosurface of CO_2 (left) and N_2 (right) molecules [58]. Reproduced with permission. Copyright 2022 Elsevier Publication. (**b**) corresponding product distributions of CO (cyan), NH_3 (grey), H_2 (blue), and urea (pink) with N_2 and CO_2 as the feed gases at various potentials using Co-PMDA-2-mbIm [59]. Reproduced with permission. Copyright 2008, RSC Publication. (**c**) The TEM and EDS mapping images of Cu^{III}-HHTP (scale bar = 200 nm). Reproduced with permission. Copyright 2023 Springer Nature Limited. (**d**) XRD pattern of CuPc NTs [62]. Reproduced with permission. Copyright 2022, WILEY Publication. (**e**) Free energy diagram for N_2CO_2RR via alternation and distal pathway on Au NSs [64]. (**f**) The SEM images of PPy coated Pt electrode [63]. Reproduced with permission. Copyright 2022, 2016 Elsevier Publication.

4. Ammonia- and Amine-Integrated CO_2 Reduction

4.1. Ammonia-Integrated CO_2 Reduction

Ammonia serves as a crucial industrial chemical with significant economic importance worldwide. In addition to the applications in the synthesis of fertilizer, disinfectant, and refrigerant, ammonia can also act as an efficient hydrogen storage medium in the hydrogen energy industry and a robust nitrogen source in electrochemical energy conversion. Therefore, several explorations were conducted for the ammonia-integrated electrocatalytic conversion of CO_2 with amides and amino acids as the most valuable products.

4.1.1. Amide Formation

Catalyzed by Cu nanoparticles on a gas diffusion layer electrode, the formation of a C-N bond was demonstrated by Jiao and co-workers through co-electrolysis of CO_2-derived CO and NH_3 [70]. Among the C-C and C-N coupling products, the acetamide can be selectively generated with nearly 40% FE (Figure 7a). According to the experimental and calculation results, after the C-C coupling between two adjacent *CO intermediates, thermodynamically favored dehydration and C-N bond formation subsequently occurred, generating acetamide as the final product. Furthermore, amines were also fitted in this C-N coupling process, yielding corresponding *N*-substituted amides with high selectivity.

Similarly, with the adaptation of a gas diffusion electrode, a C-N coupling was realized at the triple-phase boundary, where the gaseous CO_2 and liquid-phase ammonia reacted over a solid Cu catalyst [71]. Alkaline electrolytes were employed to minimize the competing HER, and the amides were detected by the NMR spectra with modest FE. Meanwhile, a thicker catalyst loading could promote the FE value for producing acetamide, while having little effect on formamide. For the generation of acetamide, the C-C coupling between reduced *CO intermediates, the dehydration, and the C-N coupling between ketene intermediate and ammonia were the crux as well. Additionally, the nitrite and nitrate ions were confirmed to be potential sources of nitrogen in this process.

4.1.2. Amino Acid Formation

Most recently, C-N bond formation between CO_2 and NH_4^+ for the synthesis of amino acids was discovered by Fang and co-workers [72]. By the fabrication of a chiral Cu film catalyst in the presence of histidine, a highly enantiomeric Serine product was obtained (Figure 7c). According to the experimental and calculation results, the 3-hydropyruvic acid was first formed through multiple C-C coupling steps. Then the amino acid was generated via the amination with ammonia. Although the electrolysis was conducted under high pressure, and a modest FE was obtained compared to formic acid and ethanol, this process undoubtedly integrates the synthesis of small biological molecules, CO_2 resource utilization, and electrochemical technology, thus offering a novel orientation for the electrochemical conversion of CO_2.

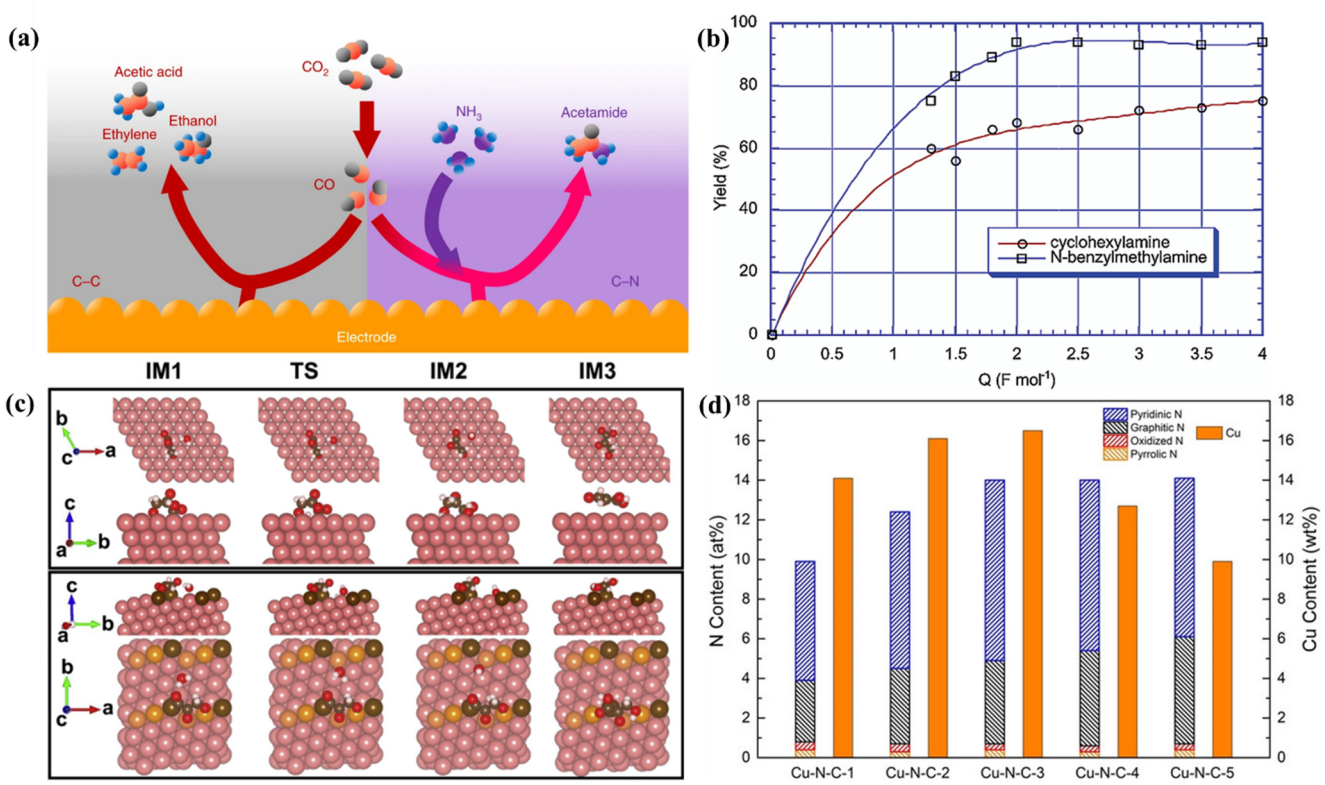

Figure 7. (**a**) Schematic diagram showing the formation of C–N bonds through the electrolysis of CO induced by ammonia [70]. Reproduced with permission. Copyright 2019 Springer Nature Limited. (**b**) Reaction of amines 1g and 1a with CO_2 and EtI in MeCN−TEAP-electrolyzed solutions. Divided cells, Pt cathode and anode, with a current density of I = 16 mA cm^{-2}. Electrolysis was carried out under constant current control. The yields (based on the starting amine) of isolated carbamates 2g and 2a versus Q (number of Faradays per mole of amines supplied to the electrodes) according to procedure A [73]. Reproduced with permission. Copyright 2003, ACS Publication. (**c**) Corresponding atomic models of transition states and intermediates in the energy curves on (111) and (653) surfaces [72]. Reproduced with permission. Copyright 2023 Elsevier Publication. (**d**) N and Cu contents in Cu-N-C materials [74]. Reproduced with permission. Copyright 2021, WILEY Publication.

4.2. Amine-Integrated CO_2 Reduction

4.2.1. Alkylation of Amines

In synthetic chemistry, when reacted with an amine, the CO_2 can act as a methylation agent to generate substituted amines. Rooney and coworkers reported that *N*-methylated products can be obtained through amine-integrated electrochemical reduction of CO_2 by phthalocyanine cobalt molecular catalysts supported by carbon nanotubes (CoPc/CNT) [75]. In 0.1 M $KHCO_3$ aqueous solution, the aniline, fatty amine, hydroxylamine, and even hydrazine were suitable nitrogen sources, while methylation does not occur with ammonium ions. It is worth noting that the *N*-methylaniline was also obtained through the co-reduction of nitrobenzene and CO_2. The C-N bond was formed by the condensation between the N nucleophile and the electrophilic $*OCH_2$, generated from the reduction of CO_2.

4.2.2. Carboxylation of Amines

As one of the promising approaches for the synthesis of carbamates, the electrochemical conversion of CO_2 with amines and alkylating reagents eliminates the use of hazardous chemicals and harsh reaction conditions, thus providing a green route for CO_2 utilization. As early as 1996, Casadei and co-workers reported the electrochemical activation of CO_2 for the synthesis of organic carbamates, a type of organic compound used in pesticides, medicines, and organic modifiers [76]. As a continuation, Faroci and co-workers proposed an efficient electrochemical synthesis of organic carbamates from $^{-}CH_2CN/CO_2$ carboxylation reagent. The reaction was conducted in the cathodic chamber of a divided cell, and the CO_2 molecules were attacked by the in-situ reduced amine intermediate (Figure 7b), namely the carboxylation of amines [73]. Thereafter, the efficiency of this procedure was further facilitated by conducting the cathodic reduction of CO_2 in ionic liquid solutions [77]. Furthermore, a combination of electrooxidation of aryl ketones and electrosynthesis of carbamates from CO_2 and amine was realized by Wang et al. [78]. The aryl ketone was first oxidized and then substituted by the in-situ generated molecular iodine. Then, the yielding organo-iodide was consumed as the alkylating agent in the electrosynthesis of carbamates. In 2021, Li and co-workers explored the catalytic performance of Cu SACs for the electrosynthesis of carbamates [74]. The Cu-N-C nanosheets were fabricated through the pyrolysis of Cu-MOF precursors (Figure 7d). The electrolysis was conducted in a divided cell under constant electric current. The optimal reaction condition was precisely screened, and the tolerance of substitutions was tested. It is reasonably speculated that the abundant high-dispersive Cu sites promoted the C-N bond formation within the catalytic mechanism.

5. Conclusions and Outlooks

Powered by sustainable energy sources, ambient-temperature electrocatalytic synthesis of functionalized organic compounds through nitrogen-assisted CO_2 transformation represents a green and energy-efficient approach. This comprehensive review systematically examines recent breakthroughs in CO_2 electroreduction facilitated by diverse nitrogen-containing precursors for selective C-N coupling. Diverse products can be obtained efficiently and selectively, such as urea, amine, amide, carbamate, and amino acids. For their generation, types of nano-engineered electrocatalysts with specific effectiveness and robustness were also demonstrated. Furthermore, the mechanisms of C-N coupling varied depending on the nitrogen-containing substrates and reaction conditions. For instance, the C-N bond formation was enabled from $*CO_2$ and $*NO_2$ to form the key $*CO_2NO_2$ intermediate for further protonation and reduction. Furthermore, the reduced *CO or *COOH could also directly couple with protonated $*NH_2$. In some cases, the C-N coupling emerged from the interaction between the *CO and $*N_2$ or released CO, generating *NCON* intermediate for subsequent hydrogenation. The C-C coupling took place before the C-N bond formation step for multiple-carbon-containing products, such as acetamide and amino acid. Meanwhile, to harvest products with higher value, exogenous auxiliary strategies were also used, like high-pressure and light irradiation. Moreover, CO_2 can also act as C1 building blocks for the decoration of amines, generating alkylation or carboxylation products under electrocatalysis conditions.

Although the electrocatalytic CO_2 reduction reaction during the experimental stage could operate stably at a current density of 100 $mA \cdot cm^{-2}$ for over 1000 h [79], with an FE efficiency exceeding 88.5% [80], there are still challenges that need to be overcome for the industrial application of electrochemical CO_2 conversion [81]. For instance, competitive side reactions, such as CO, H_2, NH_3 generation, as well as C-C bond formation were inevitable, especially under high overpotential and high operation current density. On the other hand, the precisely manufactured electrocatalysts have been costly and insufficiently stable to date. Therefore, the emerging technology of CO_2 conversion through electrocatalytic C-N coupling still demands robust efficiency and outstanding selectivity.

As revealed by previous works, nanoengineering of electrocatalysts plays an important role in constructing multifunctional catalytic active sites to precisely control reaction pathways. The synergy effects are essential for the activation of inert molecules and stabilization of key intermediates, thereby the realization of C-N bond formation. Beyond material innovation, integrating computational modeling with machine learning approaches can accelerate the design of higher-performance catalysts and more efficient reaction pathways. Besides, the details of plausible reaction mechanisms can also be influenced by the optimization of electrolytes, thus resulting in complex difficulties for the exploration of the actual pathway toward desired C-N coupling products. In this manner, *in-situ* characterization technologies could provide us with more detailed information on the reaction mechanism, which may offer abundant evidence for the improvement of catalysts. It is worth noting that several intermediates mentioned in the DFT calculations were not observed in the in-situ spectroscopic measurements. Therefore, to practically realize the industrial application of CO_2 conversion through the electrocatalytic C-N coupling technique requires more attention and dedication in the investigation of the fabrication of functional catalysts and the identification of key intermediates.

Acknowledgments

We express our thanks for funding support from the Fundamental Research Funds for Public Universities in Liaoning (LJ232410140033), the Open Foundation of State Key Laboratory of Biobased Transportation Fuel Technology, Zhejiang University (2025-002), Natural Science Foundation of Liaoning Province (general program) (2020-MS-137).

Author Contributions

Y.G.: Writing—Initial draft, research, form analysis. Z.L.: Review and edit the written content. L.Z.: Review and edit the written content, conduct research. D.F.: Review and edit the written content, supervise, manage resources, project management, secure funding, concept conception. C.G.: supervise, manage resources, project management.

Ethics Statement

Not applicable.

Informed Consent Statement

Not applicable.

Funding

This research was funded by the Fundamental Research Funds for Public Universities in Liaoning (LJ232410140033), the Open Foundation of State Key Laboratory of Biobased Transportation Fuel Technology, Zhejiang University (2025-002), Natural Science Foundation of Liaoning Province (general program) (2020-MS-137).

Declaration of Competing Interest

The author declares that at present, there are no potential conflicts of interest or personal relationships that could affect the research results reported in this article.

References

1. Ji X, Verspagen JMH, Van de Waal DB, Rost B, Huisman J. Phenotypic plasticity of carbon fixation stimulates cyanobacterial blooms at elevated CO_2. *Sci. Adv.* **2020**, *6*, eaax2926. doi:10.1126/sciadv.aax2926.
2. Davis SJ, Lewis NS, Shaner M, Aggarwal S, Arent D, Azevedo IL, et al. Net-zero emissions energy systems. *Science* **2018**, *360*, eaas9793. doi:10.1126/science.aas9793.
3. Centi G, Quadrelli EA, Perathoner S. Catalysis for CO_2 conversion: a key technology for rapid introduction of renewable energy in the value chain of chemical industries. *Energy & Environmental Science* **2013**, *6*, 1711–1731. doi:10.1039/C3EE00056G.
4. De Luna P, Hahn C, Higgins D, Jaffer SA, Jaramillo TF, Sargent EH. What would it take for renewably powered electrosynthesis to displace petrochemical processes? *Science* **2019**, *364*, eaav3506. doi:10.1126/science.aav3506.
5. Qiao J, Liu Y, Hong F, Zhang J. A review of catalysts for the electroreduction of carbon dioxide to produce low-carbon fuels. *Chem. Soc. Rev.* **2014**, *43*, 631–675. doi:10.1039/C3CS60323G.
6. Feng D-M, Zhu Y-P, Chen P, Ma T-Y. Recent Advances in Transition-Metal-Mediated Electrocatalytic CO_2 Reduction: From Homogeneous to Heterogeneous Systems. *Catalysts* **2017**, *7*, 373.
7. Spinner NS, Vega JA, Mustain WE. Recent progress in the electrochemical conversion and utilization of CO_2. *Catal. Sci. Technol.* **2012**, *2*, 19–28. doi:10.1039/C1CY00314C.
8. Tang C, Zheng Y, Jaroniec M, Qiao S-Z. Electrocatalytic Refinery for Sustainable Production of Fuels and Chemicals. *Angew. Chem. Int. Ed.* **2021**, *60*, 19572–19590. doi:10.1002/anie.202101522.
9. Kyriakou V, Garagounis I, Vourros A, Vasileiou E, Stoukides M. An Electrochemical Haber-Bosch Process. *Joule* **2020**, *4*, 142–158. doi:10.1016/j.joule.2019.10.006.
10. van Langevelde PH, Katsounaros I, Koper MTM. Electrocatalytic Nitrate Reduction for Sustainable Ammonia Production. *Joule* **2021**, *5*, 290–294. doi:10.1016/j.joule.2020.12.025.
11. Zhang X, Wang Y, Liu C, Yu Y, Lu S, Zhang B. Recent advances in non-noble metal electrocatalysts for nitrate reduction. *Chem. Eng. J.* **2021**, *403*, 126269. doi:10.1016/j.cej.2020.126269.
12. Zhang X, Wang Y, Wang Y, Guo Y, Xie X, Yu Y, et al. Recent advances in electrocatalytic nitrite reduction. *Chem. Commun.* **2022**, *58*, 2777–2787. doi:10.1039/D1CC06690K.

13. Yang C, Zhu Y, Liu J, Qin Y, Wang H, Liu H, et al. Defect engineering for electrochemical nitrogen reduction reaction to ammonia. *Nano Energy* **2020**, *77*, 105126. doi:10.1016/j.nanoen.2020.105126.
14. Suryanto BHR, Du H-L, Wang D, Chen J, Simonov AN, MacFarlane DR. Challenges and prospects in the catalysis of electroreduction of nitrogen to ammonia. *Nat. Catal.* **2019**, *2*, 290–296. doi:10.1038/s41929-019-0252-4.
15. Li Y, Wang H, Priest C, Li S, Xu P, Wu G. Advanced Electrocatalysis for Energy and Environmental Sustainability via Water and Nitrogen Reactions. *Adv. Mater.* **2021**, *33*, 2000381. doi:10.1002/adma.202000381.
16. Chen S, Liu X, Xiong J, Mi L, Song X-Z, Li Y. Defect and interface engineering in metal sulfide catalysts for the electrocatalytic nitrogen reduction reaction: a review. *J. Mater. Chem. A* **2022**, *10*, 6927–6949. doi:10.1039/D2TA00070A.
17. Li J, Zhang Y, Kuruvinashetti K, Kornienko N. Construction of C–N bonds from small-molecule precursors through heterogeneous electrocatalysis. *Nat. Rev. Chem.* **2022**, *6*, 303–319. doi:10.1038/s41570-022-00379-5.
18. Mei Z, Zhou Y, Lv W, Tong S, Yang X, Chen L, et al. Recent Progress in Electrocatalytic Urea Synthesis under Ambient Conditions. *ACS Sustain. Chem. Eng.* **2022**, *10*, 12477–12496. doi:10.1021/acssuschemeng.2c03681.
19. Patil SB, Wang D-Y. Electrochemical reactions towards the formation of heteroatomic bonds beyond CO_2 and N_2 reduction. *Sustain. Energy Fuels* **2022**, *6*, 3283–3303. doi:10.1039/D2SE00284A.
20. Shibata M, Yoshida K, Furuya N. Electrochemical synthesis of urea at gas-diffusion electrodes: Part II. Simultaneous reduction of carbon dioxide and nitrite ions at Cu, Ag and Au catalysts. *J. Electroanal. Chem.* **1998**, *442*, 67–72. doi:10.1016/S0022-0728(97)00504-4.
21. Shibata M, Furuya N. Electrochemical synthesis of urea at gas-diffusion electrodes: Part VI. Simultaneous reduction of carbon dioxide and nitrite ions with various metallophthalocyanine catalysts. *J. Electroanal. Chem.* **2001**, *507*, 177–184. doi:10.1016/S0022-0728(01)00363-1.
22. Shibata M, Yoshida K, Furuya N. Electrochemical Synthesis of Urea at Gas-diffusion Electrodes V. Simultaneous Reduction of Carbon Dioxide and Nitrite Ions with Various Boride Catalysts. *Denki Kagaku Oyobi Kogyo Butsuri Kagaku* **1998**, *66*, 584–589. doi:10.5796/kogyobutsurikagaku.66.584.
23. Shibata M, Furuya N. Simultaneous reduction of carbon dioxide and nitrate ions at gas-diffusion electrodes with various metallophthalocyanine catalysts. *Electrochim. Acta* **2003**, *48*, 3953–3958. doi:10.1016/S0013-4686(03)00534-6.
24. Tao Z, Rooney CL, Liang Y, Wang H. Accessing Organonitrogen Compounds via C–N Coupling in Electrocatalytic CO_2 Reduction. *J. Am. Chem. Soc.* **2021**, *143*, 19630–19642. doi:10.1021/jacs.1c10714.
25. Feng Y, Yang H, Zhang Y, Huang X, Li L, Cheng T, et al. Te-Doped Pd Nanocrystal for Electrochemical Urea Production by Efficiently Coupling Carbon Dioxide Reduction with Nitrite Reduction. *Nano Lett.* **2020**, *20*, 8282–8289. doi:10.1021/acs.nanolett.0c03400.
26. Liu S, Yin S, Wang Z, Xu Y, Li X, Wang L, et al. AuCu nanofibers for electrosynthesis of urea from carbon dioxide and nitrite. *Cell Rep. Phys. Sci.* **2022**, *3*, 100869. doi:10.1016/j.xcrp.2022.100869.
27. Wang H, Jiang Y, Li S, Gou F, Liu X, Jiang Y, et al. Realizing efficient C-N coupling via electrochemical co-reduction of CO_2 and NO_3^- on AuPd nanoalloy to form urea: Key C-N coupling intermediates. *Appl. Catal. B Environ.* **2022**, *318*, 121819. doi:10.1016/j.apcatb.2022.121819.
28. Krzywda PM, Paradelo Rodríguez A, Benes NE, Mei BT, Mul G. Carbon-nitrogen bond formation on Cu electrodes during CO_2 reduction in NO_3^- solution. *Appl. Catal. B Environ.* **2022**, *316*, 121512. doi:10.1016/j.apcatb.2022.121512.
29. Meng N, Ma X, Wang C, Wang Y, Yang R, Shao J, et al. Oxide-Derived Core–Shell Cu@Zn Nanowires for Urea Electrosynthesis from Carbon Dioxide and Nitrate in Water. *ACS Nano* **2022**, *16*, 9095–9104. doi:10.1021/acsnano.2c01177.
30. Saravanakumar D, Song J, Lee S, Hur NH, Shin W. Electrocatalytic Conversion of Carbon Dioxide and Nitrate Ions to Urea by a Titania–Nafion Composite Electrode. *ChemSusChem* **2017**, *10*, 3999–4003. doi:10.1002/cssc.201701448.
31. Liu X, Jiao Y, Zheng Y, Jaroniec M, Qiao S-Z. Mechanism of C-N bonds formation in electrocatalytic urea production revealed by ab initio molecular dynamics simulation. *Nat. Commun.* **2022**, *13*, 5471. doi:10.1038/s41467-022-33258-0.
32. Yang G-L, Hsieh C-T, Ho Y-S, Kuo T-C, Kwon Y, Lu Q, et al. Gaseous CO_2 Coupling with N-Containing Intermediates for Key C–N Bond Formation during Urea Production from Coelectrolysis over Cu. *ACS Catal.* **2022**, *12*, 11494–11504. doi:10.1021/acscatal.2c02346.
33. Huang Y, Yang R, Wang C, Meng N, Shi Y, Yu Y, et al. Direct Electrosynthesis of Urea from Carbon Dioxide and Nitric Oxide. *ACS Energy Lett.* **2022**, *7*, 284–291. doi:10.1021/acsenergylett.1c02471.
34. Siva P, Prabu P, Selvam M, Karthik S, Rajendran V. Electrocatalytic conversion of carbon dioxide to urea on nano-$FeTiO_3$ surface. *Ionics* **2017**, *23*, 1871–1878. doi:10.1007/s11581-017-1985-1.
35. Anastasiadou D, Costa Figueiredo M. Electrocatalytic Pathways to the Formation of C–N Bonds. *ACS Catal.* **2024**, *14*, 5088–5097. doi:10.1021/acscatal.3c04912.
36. Meng N, Huang Y, Liu Y, Yu Y, Zhang B. Electrosynthesis of urea from nitrite and CO_2 over oxygen vacancy-rich ZnO porous nanosheets. *Cell Rep. Phys. Sci.* **2021**, *2*, 100378. doi:10.1016/j.xcrp.2021.100378.
37. Cao N, Quan Y, Guan A, Yang C, Ji Y, Zhang L, et al. Oxygen vacancies enhanced cooperative electrocatalytic reduction of carbon dioxide and nitrite ions to urea. *J. Colloid Interface Sci.* **2020**, *577*, 109–114. doi:10.1016/j.jcis.2020.05.014.
38. Wei X, Wen X, Liu Y, Chen C, Xie C, Wang D, et al. Oxygen Vacancy-Mediated Selective C–N Coupling toward

Electrocatalytic Urea Synthesis. *J. Am. Chem. Soc.* **2022**, *144*, 11530–11535. doi:10.1021/jacs.2c03452.
39. Lv C, Zhong L, Liu H, Fang Z, Yan C, Chen M, et al. Selective electrocatalytic synthesis of urea with nitrate and carbon dioxide. *Nat. Sustain.* **2021**, *4*, 868–876. doi:10.1038/s41893-021-00741-3.
40. Lv C, Lee C, Zhong L, Liu H, Liu J, Yang L, et al. A Defect Engineered Electrocatalyst that Promotes High-Efficiency Urea Synthesis under Ambient Conditions. *ACS Nano* **2022**, *16*, 8213–8222. doi:10.1021/acsnano.2c01956.
41. Leverett J, Tran-Phu T, Yuwono JA, Kumar P, Kim C, Zhai Q, et al. Tuning the Coordination Structure of Cu—N—C Single Atom Catalysts for Simultaneous Electrochemical Reduction of CO_2 and NO_3^- to Urea. *Adv. Energy Mater.* **2022**, *12*, 2201500. doi:10.1002/aenm.202201500.
42. Zhang X, Zhu X, Bo S, Chen C, Qiu M, Wei X, et al. Identifying and tailoring C–N coupling site for efficient urea synthesis over diatomic Fe–Ni catalyst. *Nat. Commun.* **2022**, *13*, 5337. doi:10.1038/s41467-022-33066-6.
43. Wu Y, Jiang Z, Lin Z, Liang Y, Wang H. Direct electrosynthesis of methylamine from carbon dioxide and nitrate. *Nat. Sustain.* **2021**, *4*, 725–730. doi:10.1038/s41893-021-00705-7.
44. Tao Z, Wu Y, Wu Z, Shang B, Rooney C, Wang H. Cascade electrocatalytic reduction of carbon dioxide and nitrate to ethylamine. *J. Energy Chem.* **2022**, *65*, 367–370. doi:10.1016/j.jechem.2021.06.007.
45. Guo C, Zhou W, Lan X, Wang Y, Li T, Han S, et al. Electrochemical Upgrading of Formic Acid to Formamide via Coupling Nitrite Co-Reduction. *J. Am. Chem. Soc.* **2022**, *144*, 16006–16011. doi:10.1021/jacs.2c05660.
46. Kim JE, Jang JH, Lee KM, Balamurugan M, Jo YI, Lee MY, et al. Electrochemical Synthesis of Glycine from Oxalic Acid and Nitrate. *Angew. Chem. Int. Ed.* **2021**, *60*, 21943–21951. doi:10.1002/anie.202108352.
47. Feng D, Zhang X, Sun Y, Ma T. Surface-defective FeS_2 for electrochemical NH3 production under ambient conditions. *Nano Mater. Sci.* **2020**, *2*, 132–139. doi:10.1016/j.nanoms.2019.07.002.
48. Sun Y, Wang Y, Li H, Zhang W, Song X-M, Feng D-M, et al. Main group metal elements for ambient-condition electrochemical nitrogen reduction. *J. Energy Chem.* **2021**, *62*, 51–70. doi:10.1016/j.jechem.2021.03.001.
49. Feng D-M, Sun Y, Yuan Z-Y, Fu Y, Jia B, Li H, et al. Ampoule method fabricated sulfur vacancy-rich N-doped ZnS electrodes for ammonia production in alkaline media. *Mater. Renew. Sustain. Energy* **2021**, *10*, 8. doi:10.1007/s40243-021-00193-x.
50. Sun Y, Deng Z, Song X-M, Li H, Huang Z, Zhao Q, et al. Bismuth-Based Free-Standing Electrodes for Ambient-Condition Ammonia Production in Neutral Media. *Nano-Micro Lett.* **2020**, *12*, 133. doi:10.1007/s40820-020-00444-y.
51. Li D, Xu N, Zhao Y, Zhou C, Zhang L-P, Wu L-Z, et al. A Reliable and Precise Protocol for Urea Quantification in Photo/Electrocatalysis. *Small Methods* **2022**, *6*, 2200561. doi:10.1002/smtd.202200561.
52. Ma W, He X, Wang W, Xie S, Zhang Q, Wang Y. Electrocatalytic reduction of CO_2 and CO to multi-carbon compounds over Cu-based catalysts. *Chem. Soc. Rev.* **2021**, *50*, 12897–12914. doi:10.1039/D1CS00535A.
53. Chen C, Zhu X, Wen X, Zhou Y, Zhou L, Li H, et al. Coupling N_2 and CO_2 in H_2O to synthesize urea under ambient conditions. *Nat. Chem.* **2020**, *12*, 717–724. doi:10.1038/s41557-020-0481-9.
54. Wu W, Yang Y, Wang Y, Lu T, Dong Q, Zhao J, et al. Boosting electrosynthesis of urea from N_2 and CO_2 by defective Cu-Bi. *Chem Catal.* **2022**, *2*, 3225–3238. doi:10.1016/j.checat.2022.09.012.
55. Yuan M, Chen J, Bai Y, Liu Z, Zhang J, Zhao T, et al. Unveiling Electrochemical Urea Synthesis by Co-Activation of CO_2 and N_2 with Mott–Schottky Heterostructure Catalysts. *Angew. Chem. Int. Ed.* **2021**, *60*, 10910–10918. doi:10.1002/anie.202101275.
56. Yuan M, Chen J, Bai Y, Liu Z, Zhang J, Zhao T, et al. Electrochemical C–N coupling with perovskite hybrids toward efficient urea synthesis. *Chem. Sci.* **2021**, *12*, 6048–6058. doi:10.1039/D1SC01467F.
57. Yuan M, Chen J, Xu Y, Liu R, Zhao T, Zhang J, et al. Highly selective electroreduction of N_2 and CO_2 to urea over artificial frustrated Lewis pairs. *Energy Environ. Sci.* **2021**, *14*, 6605–6615. doi:10.1039/D1EE02485J.
58. Yuan M, Zhang H, Xu Y, Liu R, Wang R, Zhao T, et al. Artificial frustrated Lewis pairs facilitating the electrochemical N_2 and CO_2 conversion to urea. *Chem Catal.* **2022**, *2*, 309–320. doi:10.1016/j.checat.2021.11.009.
59. Yuan M, Chen J, Zhang H, Li Q, Zhou L, Yang C, et al. Host–guest molecular interaction promoted urea electrosynthesis over a precisely designed conductive metal–organic framework. *Energy Environ. Sci.* **2022**, *15*, 2084–2095. doi:10.1039/D1EE03918K.
60. Gao Y, Wang J, Yang Y, Wang J, Zhang C, Wang X, et al. Engineering Spin States of Isolated Copper Species in a Metal–Organic Framework Improves Urea Electrosynthesis. *Nano-Micro Lett.* **2023**, *15*, 158. doi:10.1007/s40820-023-01127-0.
61. Yang S, Yu Y, Gao X, Zhang Z, Wang F. Recent advances in electrocatalysis with phthalocyanines. *Chem. Soc. Rev.* **2021**, *50*, 12985–13011. doi:10.1039/D0CS01605E.
62. Mukherjee J, Paul S, Adalder A, Kapse S, Thapa R, Mandal S, et al. Understanding the Site-Selective Electrocatalytic Co-Reduction Mechanism for Green Urea Synthesis Using Copper Phthalocyanine Nanotubes. *Adv. Funct. Mater.* **2022**, *32*, 2200882. doi:10.1002/adfm.202200882.
63. Kayan DB, Köleli F. Simultaneous electrocatalytic reduction of dinitrogen and carbon dioxide on conducting polymer electrodes. *Appl. Catal. B Environ.* **2016**, *181*, 88–93. doi:10.1016/j.apcatb.2015.07.045.
64. Bharath G, Karthikeyan G, Kumar A, Prakash J, Venkatasubbu D, Kumar Nadda A, et al. Surface engineering of Au nanostructures for plasmon-enhanced electrochemical reduction of N_2 and CO_2 into urea in the visible-NIR region. *Appl.*

Energy **2022**, *318*, 119244. doi:10.1016/j.apenergy.2022.119244.
65. Zhu X, Zhou X, Jing Y, Li Y. Electrochemical synthesis of urea on MBenes. *Nat. Commun.* **2021**, *12*, 4080. doi:10.1038/s41467-021-24400-5.
66. Zhu C, Wen C, Wang M, Zhang M, Geng Y, Su Z. Non-metal boron atoms on a CuB12 monolayer as efficient catalytic sites for urea production. *Chem. Sci.* **2022**, *13*, 1342–1354. doi:10.1039/D1SC04845G.
67. Roy P, Pramanik A, Sarkar P. Dual-Silicon-Doped Graphitic Carbon Nitride Sheet: An Efficient Metal-Free Electrocatalyst for Urea Synthesis. *J. Phys. Chem. Lett.* **2021**, *12*, 10837–10844. doi:10.1021/acs.jpclett.1c03242.
68. Zhang Z, Guo L. Electrochemical reduction of CO_2 and N_2 to synthesize urea on metal–nitrogen-doped carbon catalysts: a theoretical study. *Dalton Trans.* **2021**, *50*, 11158–11166. doi:10.1039/D1DT01390D.
69. Zhu C, Wang M, Wen C, Zhang M, Geng Y, Zhu G, et al. Establishing the Principal Descriptor for Electrochemical Urea Production via the Dispersed Dual-Metals Anchored on the N-Decorated Graphene. *Adv. Sci.* **2022**, *9*, 2105697. doi:10.1002/ad*vs.*202105697.
70. Jouny M, Lv J-J, Cheng T, Ko BH, Zhu J-J, Goddard WA, et al. Formation of carbon–nitrogen bonds in carbon monoxide electrolysis. *Nat. Chem.* **2019**, *11*, 846–851. doi:10.1038/s41557-019-0312-z.
71. Li J, Kornienko N. Electrochemically driven C–N bond formation from CO_2 and ammonia at the triple-phase boundary. *Chem. Sci.* **2022**, *13*, 3957–3964. doi:10.1039/D1SC06590D.
72. Fang Y, Liu X, Liu Z, Han L, Ai J, Zhao G, et al. Synthesis of amino acids by electrocatalytic reduction of CO_2 on chiral Cu surfaces. *Chem* **2023**, *9*, 460–471. doi:10.1016/j.chempr.2022.10.017.
73. Feroci M, Casadei MA, Orsini M, Palombi L, Inesi A. Cyanomethyl Anion/Carbon Dioxide System: An Electrogenerated Carboxylating Reagent. Synthesis of Carbamates under Mild and Safe Conditions. *J. Org. Chem.* **2003**, *68*, 1548–1551. doi:10.1021/jo0266036.
74. Li S-M, Shi Y, Zhang J-J, Wang Y, Wang H, Lu J-X. Atomically Dispersed Copper on N-Doped Carbon Nanosheets for Electrocatalytic Synthesis of Carbamates from CO_2 as a C1 Source. *ChemSusChem* **2021**, *14*, 2050–2055. doi:10.1002/cssc.202100342.
75. Rooney CL, Wu Y, Tao Z, Wang H. Electrochemical Reductive N-Methylation with CO_2 Enabled by a Molecular Catalyst. *J. Am. Chem. Soc.* **2021**, *143*, 19983–19991. doi:10.1021/jacs.1c10863.
76. Casadei MA, Inesi A, Moracci FM, Rossi L. Electrochemical activation of carbon dioxide: Synthesis of carbamates. *Chem. Commun.* **1996**, *22*, 2575–2576. doi:10.1039/CC9960002575.
77. Feroci M, Orsini M, Rossi L, Sotgiu G, Inesi A. Electrochemically Promoted C−N Bond Formation from Amines and CO_2 in Ionic Liquid BMIm−BF4: Synthesis of Carbamates. *J. Org. Chem.* **2007**, *72*, 200–203. doi:10.1021/jo061997c.
78. Wang J, Qian P, Hu K, Zha Z, Wang Z. Electrocatalytic Fixation of Carbon Dioxide with Amines and Arylketones. *ChemElectroChem* **2019**, *6*, 4292–4296. doi:10.1002/celc.201801724.
79. Hao S, Elgazzar A, Ravi N, Wi T-U, Zhu P, Feng Y, et al. Improving the operational stability of electrochemical CO_2 reduction reaction via salt precipitation understanding and management. *Nat. Energy* **2025**, *10*, 266–277. doi:10.1038/s41560-024-01695-4.
80. Zhao C, Jin Y, Yuan J, Hou Q, Li H, Yan X, et al. Tailoring Activation Intermediates of CO_2 Initiates C–N Coupling for Highly Selective Urea Electrosynthesis. *J. Am. Chem. Soc.* **2025**, *147*, 8871–8880. doi:10.1021/jacs.5c00583.
81. Karamad M. Insights into C–N Bond Formation through the Coreduction of Nitrite and CO_2: Guiding Selectivity Toward C–N Bond. *ACS Catal.* **2025**, *15*, 8497–8510. doi:10.1021/acscatal.4c07724.